Letter

Spin-projected charge conductance in SNN junctions with noncentrosymmetric superconductors

T. H. Kokkeler [1,2,*] Y. Tanaka,[3] and A. A. Golubov[2]

[1]*Donostia International Physics Center, 20018 Donostia–San Sebastian, Spain*
[2]*Interfaces and Correlated Electron Systems, Faculty of Science and Technology, University of Twente, Enschede, The Netherlands*
[3]*Department of Applied Physics, Nagoya University, Nagoya 464-8603, Japan*

A superconductor–normal-metal–normal-metal junction in which the superconducting potential is a mixture between s-wave and p-wave potentials is investigated using the Usadel equation equipped with Tanaka-Nazarov boundary conditions. This Research Letter provides several ways to distinguish between s-wave+chiral p-wave superconductors and s-wave+helical p-wave superconductors and a way to determine whether a superconductor has a mixed pair potential. Thus it is of great importance in the determination of the pair potential of superconductors. It is shown that the different spin sectors satisfy independent equations and can thus be calculated separately even if the d vector depends on the direction of momentum. This greatly simplifies the equations to be solved. It was found that a difference in conductance for sectors with opposite spins arises if both an s-wave component and a p-wave component are present, even in the absence of a magnetic field. It is shown that the spin-projected charge conductance for s-wave + chiral p-wave junctions and s-wave + helical p-wave junctions is qualitatively similar. A setup containing two superconductor–normal-metal junctions is shown to give a clear difference between the two types of superconductivity.

The field of superconductivity has attracted a lot of attention since its discovery, both experimentally and theoretically [1]. Since the discovery of high-temperature superconductors [2–4] and the discovery of novel types of materials such as topological insulators [5], attention has shifted more and more towards unconventional superconductors [6–10], such as spin-triplet superconductors [11,12], whose existence remains under debate even today [7,13], and odd-frequency superconductivity [14–17]. Many efforts focus on superconductors whose crystal has inversion symmetry, with pair potentials that have a well-defined parity. However, if the underlying crystal of a superconductor breaks inversion symmetry, the resulting pair potential is expected to be of mixed parity [18]. There have been discovered several superconductors whose crystal possesses inversion symmetry breaking [19–29].

Whereas there has been an effort to understand the proximity effect induced by these materials [30], a good understanding of the charge transport in structures containing noncentrosymmetric superconductors is still lacking. Moreover, little is known about how to distinguish between different types of mixed-parity superconductors.

In this Research Letter we theoretically investigate the charge conductance and spin-projected charge conductance of mixed-parity superconductors and propose an experiment using which different types of mixed pair potentials can be distinguished. The experiment we propose based on our model can be used to narrow the window of possible pair potentials of unconventional superconductors.

Mixed potentials in a superconductor–normal-metal–normal-metal (SNN) junction were studied in the one-dimensional (1D) case using a form [31] of the Tanaka-Nazarov boundary conditions. However, in the one-dimensional case, one cannot distinguish between different types of s-wave+p-wave potentials. The 1D Fermi surface consists of only two points; so there is only one even (s) and one odd (p) mode. Therefore, in this Research Letter the method is generalized to the two-dimensional s-wave+chiral p-wave junctions and s-wave+helical p-wave junctions (Fig. 1). Moreover, the expression for the resistance of the junction following from the Keldysh equations [31] has been generalized, allowing the distribution functions to be opposite for opposite spins.

It is shown that the density of states, the charge conductance, and the spin-projected charge conductance can all be used to distinguish between s-wave+chiral p-wave superconductors and s-wave+helical p-wave superconductors. In addition, it is shown that the spin-projected charge conductance can be used to determine whether a superconductor has a mixed pair potential. With this, this Research Letter contributes to the determination of pair potentials in and the understanding of novel unconventional superconductors.

This Research Letter is organized as follows. First, we describe the method that we use to model the system and how to deduce the density of states and conductance from our results. Then we show the results for junctions with s-wave+helical p-wave superconductors and s-wave+chiral
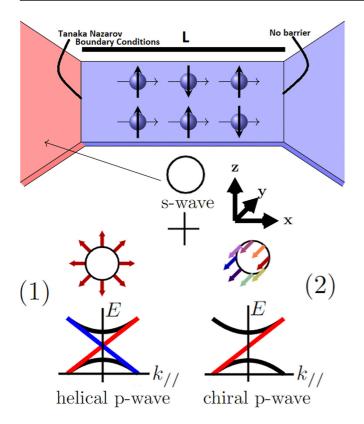
---

*tim.kokkeler@dipc.org

FIG. 1. Illustration of the SNN junction investigated in this Research Letter, with the normal metal bar between the two reservoirs. The superconductor is indicated with a red color, whereas normal metals are blue. Using a superconductor with a mixed singlet (s-wave) and triplet (p-wave) pair potential leads to a difference in conductance for opposite spins in the SNN junction. Two types of superconducting pair potential are investigated. First, superconductors having a pair potential with a mixture of s-wave and helical p-wave [Eq. (2)] components are investigated. For helical superconductors the magnitude and phase of the d vector are constant, but the direction of the d vector is aligned with the direction of momentum. In helical superconductors there are two sets of chiral edge modes, the left- and right-traveling modes. Second, superconductors having a pair potential with a mixture of s-wave and chiral p-wave [Eq. (3)] components are investigated. For chiral superconductors the d vector always points out-of-plane but has a phase dependent on the direction of momentum, as illustrated by color. The bulk-boundary correspondence implies that for chiral superconductors there is only one type of chiral edge modes, only the right-moving edge states or only the left-moving edge states.

p-wave superconductors. We conclude with a summary of the results and an outlook.

A conventional way to describe mesoscopic systems that include superconductors is using the quasiclassical Keldysh Green's function technique [32,33], where the Green's function is given by $G = \begin{bmatrix} G^R & G^K \\ 0 & G^A \end{bmatrix}$, where G^R, G^A, and G^K are the retarded, advanced, and Keldysh Green's functions in particle-hole and spin space. The Eilenberger equation [34,35] is used in the clean limit, and the Usadel equation [36] is used in the dirty limit. The Usadel equation reads

$$\nabla(G\nabla G) = [iE\tau_3, G], \qquad (1)$$

where E is the energy and τ_3, a 4×4 matrix, is the third Pauli matrix in Nambu space. In this Research Letter, the Usadel equation will be studied to describe a normal metal in proximity [37–48] to a superconductor whose pair potential has both an s-wave component and a p-wave component, studied before in different geometries and limits [30,49–52]. The geometry to be studied is a superconductor–normal-metal–normal-metal junction (SNN junction). We will model the normal metal bar in the middle and treat the other parts as superconducting and normal metal reservoirs, respectively.

It is assumed that the contact with the normal metal electrode is very good. Therefore continuity at this interface can be assumed. At the interface between the bar and the superconducting electrode, the Usadel equation is equipped with the Tanaka-Nazarov boundary conditions [53]. The Tanaka-Nazarov boundary conditions are the generalization of Nazarov's circuit theory [54] to non-isotropic superconductors, using the fact that odd-parity even-frequency triplet superconductors may induce even-parity odd-frequency triplet pairs in a dirty normal metal [55]. Using these boundary conditions, several types of systems have been studied [56–63].

In Ref. [31] a form of the Tanaka-Nazarov boundary conditions was derived, and this form was used to study one-dimensional SNN junctions. In addition to the one-dimensional bar, a two-dimensional bar in which the Green's function has no y dependence can also be considered, that is, either a bar that is thin enough that the one-dimensional Usadel equation can be studied or a junction that is wide, so that boundaries are far away. In this case, the Usadel equation does not change, but multiple modes contribute to the Tanaka-Nazarov conditions [53,54,56]. The modes are integrated as specified in Ref. [56]. For pairs with opposite spin, the s-wave potential changes sign, whereas the p-wave potential does not. The same parameters in the Tanaka-Nazarov boundary conditions were used as in Ref. [31]; that is, the ratio γ_B between boundary resistance and bar resistance is set to $\gamma_B = 2$, the transparency is given by $T = \frac{\cos^2 \phi}{\cos^2 \phi + z^2}$ with the barrier parameter $z = 0.75$, and the Thouless energy was set to $E_{\text{Th}} = \frac{D}{L^2} = 0.02\Delta$, where D is the diffusion constant, L is the length of the junction, and Δ is the superconducting gap.

The density of states on the normal metal side of the superconductor–normal-metal interface and the conductance of the junction were calculated for various ratios between the magnitudes of the singlet and triplet components of the pair potential. The calculation for the s-wave + chiral p-wave junction, for which the d vector is $(0, 0, e^{i\phi})$, is relatively similar to the calculation of the one-dimensional s-wave + p-wave junction, though the phase in the diffusive normal metal must be computed numerically, as discussed in the Supplemental Material. The calculation of the Green's function in the s-wave + helical p-wave junction is more complicated than for the one-dimensional case studied in Ref. [31] or the two-dimensional s-wave + p_x-wave junction and s-wave + chiral p-wave junction, because the d vector has directional dependence. For mixed s-wave and helical p-wave superconductors [64–67],

$$\bar{\Delta} = \Delta_s \mathbf{1} + \Delta_p(\cos\phi\,\sigma_x + \sin\phi\,\sigma_y), \quad \Delta_\pm = \Delta_s \pm \Delta_p, \quad (2)$$

whereas for mixed s-wave and chiral p-wave superconductors [68–70],

$$\bar{\Delta} = \Delta_s \mathbf{1} + \Delta_p e^{i\phi} \sigma_z, \quad \Delta_\pm = \Delta_s \pm \Delta_p e^{\pm i\phi}. \quad (3)$$

In both cases we define

$$\Delta_0 = \sqrt{\Delta_s^2 + \Delta_p^2}, \quad (4)$$

$$r = \frac{\Delta_p}{\Delta_s}. \quad (5)$$

The retarded Green's function is a 4×4 matrix. The Usadel equation for 4×4 matrices is much less convenient to solve than the Usadel equation for 2×2 matrices, because satisfying the normalization condition is more complex. Therefore a way to find two separated equations for 2×2 matrices, as for the previous cases, was sought.

$$G = \begin{bmatrix} \cosh\theta_\uparrow & 0 & 0 & \sinh\theta_\uparrow e^{i\chi_\uparrow} \\ 0 & \cosh\theta_\downarrow & \sinh\theta_\downarrow e^{i\chi_\downarrow} & 0 \\ 0 & -\sinh\theta_\downarrow e^{-i\chi_\downarrow} & -\cosh\theta_\downarrow & 0 \\ -\sinh\theta_\uparrow e^{-i\chi_\uparrow} & 0 & 0 & -\cosh\theta_\uparrow \end{bmatrix}, \quad (7)$$

where $\theta_{\uparrow,\downarrow}$ and $\chi_{\uparrow,\downarrow}$ are complex scalar functions of position for $0 \leqslant x \leqslant L$. In the Supplemental Material [71] it is shown that the Green's function is indeed always in this subspace, and even more, that the following relations hold for the up and down sectors: $\theta_\uparrow = -\theta_\downarrow =: \theta$, $\chi_\uparrow = -\chi_\downarrow =: \chi$. Since χ must be constant due to the absence of a supercurrent in the SNN junction, the problem is reduced to the following equation for the function $\theta(x)$ and parameter χ:

$$D\frac{d^2\theta}{dx^2} + 2iE\sinh\theta = 0, \quad (8)$$

$$\theta(x = L) = 0, \quad (9)$$

$$\frac{d\theta}{dx}\bigg|_{x=0} = S_\theta(\theta(0), \chi), \quad (10)$$

$$S_\chi(\theta(0), \chi) = 0, \quad (11)$$

where S_θ and S_χ are determined by the Tanaka-Nazarov boundary conditions. The full expression for these terms is discussed in more detail in the Supplemental Material. The density of states normalized to its value in the metallic state can be calculated from the results using

$$\rho(E) = \text{Tr}\frac{1}{2}(\mathbf{1} + \tau_3)G, \quad (12)$$

where τ_3 is the third Pauli matrix in Nambu space and $\mathbf{1}$ is the 4×4 identity matrix. The resulting local density of states normalized to the normal metal local density of states is shown in Fig. 2. If the s-wave component of the pair potential is dominant, that is, if $r < 1$, there is a dip in the density of states at zero energy, whereas $r > 1$ results in a peak in the density of states at zero energy. In contrast to a bulk superconductor, the density of states is finite for all energies because of the presence of the normal metal electrode. The zero-energy peak or dip is equally high for mixed potentials as it is for pure

For the s-wave + chiral p-wave case this separation is immediate since the equations for the different spin configurations $[\frac{1}{2}(\mathbf{1} \pm \sigma_z)]$ are decoupled. For the s-wave + helical p-wave case, however, this is less clear in advance since the spin direction depends on the direction of momentum. From expression (2) it is found that the average potential over $(-\frac{\pi}{2}, \frac{\pi}{2})$ is $\Delta_s + \frac{2}{\pi}\Delta_p\sigma_x$. Thus it is convenient to transform to the basis of spins polarized in the x direction via $G \to UGU$, where

$$U = \frac{1}{\sqrt{2}}\begin{bmatrix} \sigma_x + \sigma_z & 0 \\ 0 & \sigma_x + \sigma_z \end{bmatrix}. \quad (6)$$

Since $U\tau_3 U = \tau_3$ and U^2 is the identity, this Green's function satisfies the Usadel equation with Tanaka-Nazarov boundary conditions if G_S is also transformed to $UG_S U$. It will be shown that after this transformation, G is of the form

s-wave or helical p-wave superconductors, similar to the one-dimensional case [31].

This can be understood from Eqs. (2) and (3). In contrast to the chiral p-wave junctions, the potentials $\Delta_\pm$ are independent of angle for helical p-wave junctions. This independence arises because the eigenvalues of $(\cos\phi\sigma_x + \sin\phi\sigma_y)$ are always 1 and −1, regardless of ϕ. Therefore $\frac{\Delta_+}{|\Delta_+|}$ is 1 and $\frac{\Delta_-}{|\Delta_-|}$ is either 1 (if $r < 1$) or −1 (if $r > 1$) regardless of the angle ϕ. This should be contrasted with the chiral p-wave case, where $\Delta_\pm = \frac{1}{\sqrt{r^2+1}}(1 \pm re^{i\phi})$, which means that $\frac{\Delta_+}{|\Delta_+|}$ and $\frac{\Delta_-}{|\Delta_-|}$ will be dependent on r, ϕ.

Since the zero-energy results only depend on $\frac{\Delta_+}{|\Delta_+|}$ and $\frac{\Delta_-}{|\Delta_-|}$, as discussed in the Supplemental Material, there is a binary distinction at $E = 0$ between $r < 1$ and $r > 1$ for s-wave + helical p-wave superconductors and a nonbinary distinction for s-wave + chiral p-wave junctions. For nonzero energies the density of states becomes dependent on the actual value of r. For $r < 1$ there is a peak at $E \approx \Delta_-$, then the density of states slowly decays for $E \in (\Delta_-, \Delta_+)$, and a very sharp decay towards the normal states for $E > \Delta_+$ follows. If $r > 1$ there is a dip around $E \approx |\Delta_-|$, after which the density of states increases towards the normal states value.

The conductance was also calculated for the s-wave + helical p-wave superconductor. Observe that if the retarded part C^R satisfies $C^R(-\phi) = YC^R(\phi)Y$, then the advanced part C^A and Keldysh part C^K satisfy $YC^A(-\phi)Y = C^A(\phi)$ and $YC^K(-\phi)Y = C^K(\phi)$ as well.

Thus the equations for the Keldysh part also split into two systems of equations for 2×2 matrices that are coupled at the boundary. Even more, the equations $\theta_\uparrow = -\theta_\downarrow$ and $\chi_\uparrow = -\chi_\downarrow$ are still satisfied by the symmetry discussed in the Supplemental Material, as in the p_x-wave and chiral p-wave case. Thus the expression for the resistance of the junction can be derived in a similar manner to Ref. [31], with an appropriate definition of I^K. The expressions for I^K need to
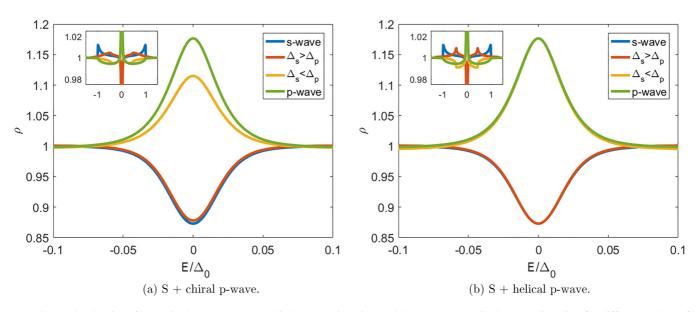
FIG. 2. The density of states in the (a) s-wave + chiral p-wave junction and (b) s-wave + helical p-wave junction for different values of $r = \frac{\Delta_p}{\Delta_s}$ as a function of energy E, $r \in \{0, 0.5, 2, \infty\}$, where $r = 0$ and $r = \infty$ correspond to s-wave and p-wave pair potentials, respectively. In the insets it is shown that there is a zero-energy peak in the density of states if the p-wave component is dominant, while there is a dip if the s-wave component is dominant, similar to the one-dimensional case [31]. Both the peak and the dip have a width of the order of the Thouless energy. For nonzero energies the density of states becomes dependent on the actual value of r. Parameters are set to $\gamma_B = 2$, $z = 0.75$, and $E_{\text{Th}} = 0.02\Delta$.

be compared with the definition in Ref. [31]. The definition of I^K used here is discussed in the Supplemental Material, where it is also shown that the expression found here reduces to the expression in Ref. [31] if there is no helical component in the superconducting pair potential.

The conductance is given by

$$\sigma = \frac{\partial I}{\partial V}, \tag{13}$$

$$I^K = \frac{\sigma_N}{16e} \int_{-\infty}^{\infty} dE \, \text{Tr}\{\tau_3(\bar{G}\nabla\bar{G})^K\}, \tag{14}$$

$$\sigma_{\text{up}} - \sigma_{\text{down}} = \frac{\sigma_N}{16e} \int_{-\infty}^{\infty} dE \, \text{Tr}\{\tau_3\sigma_d(\bar{G}\nabla\bar{G})^K\}, \tag{15}$$

where σ_d is a Pauli matrix determined by the direction of the d vector. For s-wave + chiral p-wave superconductors, $\sigma_d = \sigma_3$ always; for s-wave + helical p-wave superconductors, σ_d depends on the direction of the interface and can be σ_1 or σ_2. The results for the conductance are shown in Fig. 3 normalized to the conductance σ_N of the normal metal if it is not in proximity to the superconductor. Results are shown for $r = 0, \frac{1}{2}, 2, \infty$. The conductance in the s-wave + helical p-wave junction is very similar to the conductance in the s-wave + chiral p-wave junction; if $\Delta_p > \Delta_s$, there is both a sharp peak and a broader peak. This is consistent with the appearance of Andreev bound states with dispersion in Ref. [72].

An important difference compared with the s-wave + chiral p-wave junctions is that for s-wave + helical p-wave junctions the zero-bias conductance is quantized; that is, it assumes a constant value for $r < 1$ and a constant value for $r > 1$. Thus, whereas the addition of an s-wave component lowered the zero-bias conductance peak both when mixed with a p_x-wave component and when mixed with a chiral

p-wave component, in helical superconductor junctions the addition of an s-wave component does not influence the height of the zero-bias conductance peak. Moreover, the double-peak structure, as observed in Ref. [73] and discussed for pure chiral p-wave superconductors in Ref. [57], is robust against the inclusion of an s-wave component. This is in correspondence with the results for the density of states and the pair amplitude. The derivation of the conductance in the Supplemental Material explicitly allows for a difference in conductance for different spin orientations. This feature has never appeared in superconductors that are spin-singlet or spin-triplet superconductors without parity mixing; so it is expected that this difference should vanish for these types of superconductors. However, for mixed-type superconductors it is different. The Green's function has both a singlet component and a triplet component; that is, the spin structure is of the form $a + b\sigma$ with $ab \neq 0$. This means that for each angle there is a spin polarization in the Green's function. Averaged over the full angle, this polarization will disappear. However, for the boundary condition, the average is only taken over $(-\frac{\pi}{2}, \frac{\pi}{2})$, and it is not clear whether this term vanishes.

An exact expression for the spin-projected charge conductance can be found in the Supplemental Material. The spin-projected charge conductance $\sigma_{\text{up}} - \sigma_{\text{down}}$ is shown for the quasi-one-dimensional s-wave + p_x-wave junction in Fig. 4 for different values of r. It is confirmed that if the superconducting pair potential is of a pure s-wave or p-wave type, the difference in conductance for opposite spins is zero, as expected. However, if $r \in (0, \infty)$, there is a finite difference in conductance for different spins. For low voltages this difference is very small, but between $eV = |\Delta_-|$ and $eV = \Delta_+$ the spin-projected charge conductance is not small. The spin-projected charge conductance
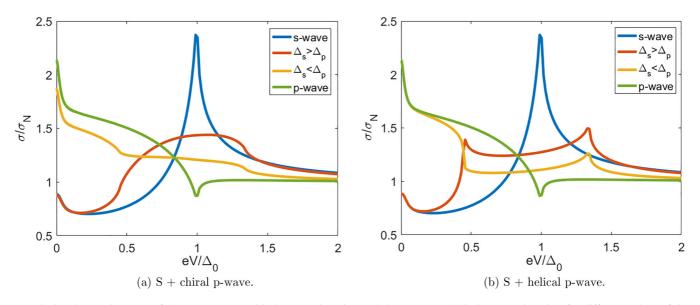
(a) S + chiral p-wave.

(b) S + helical p-wave.

FIG. 3. The conductance of the (a) s-wave + chiral p-wave junction and (b) s-wave + helical p-wave junction for different values of the parameter $r = \frac{\Delta_p}{\Delta_s}$, $r \in \{0, 0.5, 2, \infty\}$, where $r = 0$ and $r = \infty$ correspond to the s-wave and p-wave pair potentials. There is a clear zero-bias conductance peak if the p-wave component is dominant, consisting of both a contribution with a width of the order of the Thouless energy and a broad peak inherent to the dominant p-wave pair potential. If the s-wave component is dominant, there is only a small peak of the width of the Thouless energy [42]. For the s-wave + helical p-wave superconductor the zero-bias conductance peak is robust against inclusion of an s-wave component of the pair potential; for the s-wave + chiral p-wave superconductor it is not. Moreover, for $eV \in (\Delta_-, \Delta_+)$, there is a smooth peak for s-wave + chiral p-wave junctions and two sharper peaks for s-wave + helical p-wave junctions. Parameters are set to $\gamma_B = 2$, $z = 0.75$, and $E_{\mathrm{Th}} = 0.02\Delta$.

for s-wave + chiral p-wave superconducting junctions is qualitatively similar to that for s-wave + helical p-wave superconducting junctions, though for the s-wave + helical p-wave case the change around $eV = \Delta_+$ is much sharper. The spin-projected charge conductances for s-wave + chiral p-wave superconductors and s-wave + helical p-wave

superconductors are qualitatively similar. For s-wave + helical p-wave superconductors, the change at $eV \approx \Delta_+$ is much sharper than for s-wave + chiral p-wave superconductors. However, this difference might not be clearly visible in experiment due to uncertainties. However, a clear difference between s-wave + chiral p-wave superconductors and s-wave
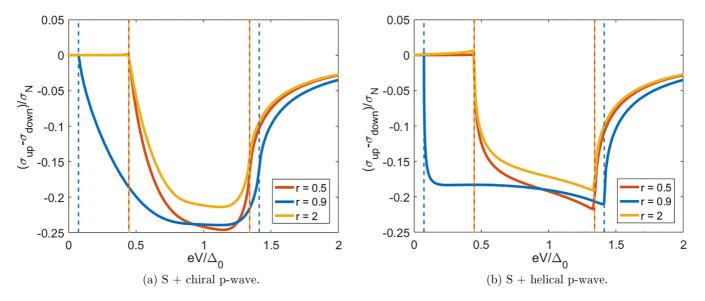

(a) S + chiral p-wave.

(b) S + helical p-wave.

FIG. 4. The spin-projected charge conductance for (a) s-wave + chiral p-wave junctions and (b) s-wave + helical p-wave junctions. For spin-singlet or spin-triplet superconductors without parity mixing, the spin-projected charge conductance is spin independent, but for mixed-potential superconductors there is a difference in the conductance for different spin orientations. The difference in spin-projected charge conductance is very small for $eV < |\Delta_-|$, indicated with the left dashed lines, and decays to zero for $eV > \Delta_+$, indicated with the right dashed lines. The results for s-wave + chiral p-wave junctions and s-wave + helical p-wave junctions are qualitatively similar, though for s-wave + helical p-wave junctions the transition between the three regimes is much sharper. Parameters are set to $\gamma_B = 2$, $z = 0.75$, and $E_{\mathrm{Th}} = 0.02\Delta$.
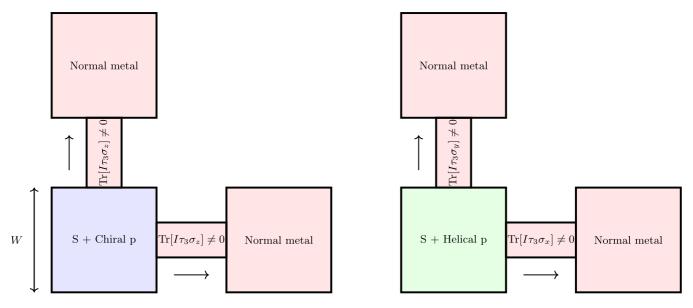
FIG. 5. Schematic of an experiment that can be used to distinguish between *s*-wave + chiral *p*-wave junctions and *s*-wave + helical *p*-wave junctions. The width W of the junction is much larger than the coherence length, so that the horizontal and vertical junctions can be ignored. For the *s*-wave + chiral *p*-wave junction the spin polarization of the current is the same in both bars, whereas for the *s*-wave + helical *p*-wave junction the polarization of the current has a perpendicular direction in one bar compared with the other.

+ helical *p*-wave superconductors can be observed in the setup in Fig. 5. Instead of using a single SNN junction, a corner junction is studied. It is assumed that the size W of the superconductor is much larger than the coherence length, so that the different arms of the junction do not influence each other and thus the two arms can be considered as separate SNN junctions rather than a single NNSNN junction.

For the *s*-wave + chiral *p*-wave superconductor the d vector points in the z direction independent of the direction of momentum; so both bars will show a difference in conductance for spins polarized in the z direction. For the *s*-wave + helical *p*-wave case, however, the d vector is dependent on the direction of momentum. In the previous sections it was shown that the spin polarization depends on the average over the Green's function over modes that make an angle less than $\frac{\pi}{2}$ with the outward normal. This means that for one of the bars the current will be partly polarized along the x direction, whereas for the other bar the current will be partly polarized along the y direction. Thus, whereas for the *s*-wave + chiral *p*-wave superconducting junction the spin polarization is in the same direction, for the *s*-wave + helical *p*-wave junction the spin polarization is in perpendicular directions. This means that a clear difference between *s*-wave + chiral *p*-wave superconductors and *s*-wave + helical *p*-wave superconductors can be observed.

In this Research Letter it has been shown that the SNN junction can be used to distinguish mixed *s*-wave + *p*-wave superconductors from the pure *s*-wave or *p*-wave superconductors. Moreover, it is shown that a spin-projected charge conductance can be used to distinguish different types of *s*-wave + *p*-wave potentials, such as *s*-wave + chiral *p*-wave potentials and *s*-wave + helical *p*-wave potentials. A form of the Tanaka-Nazarov boundary conditions was applied to

two-dimensional helical *s*-wave + *p*-wave junctions. It was shown that the equations for the helical *p*-wave junctions can be solved using the 2×2 matrix formalism, even though there is a strong coupling between the d vector and the direction of the momentum in the superconductor. This allows for the usage of the θ parametrization. Moreover, an expression for the conductance was found by allowing the distribution functions in the Keldysh component to be spin dependent. In the case of an *s*-wave or *p*-wave superconducting pair potential without parity mixing, the expression found here reduces to the known expression. In the case of a mixed potential the correction to the total conductance is only small; however, it was found that there is a difference in the conductance for different spin orientations in case both an *s*-wave component and a *p*-wave component are present in the pair potential. For future work, it is important to investigate the supercurrent in junctions containing two superconductors including *s*-wave + helical *p*-wave superconductivity and to calculate whether dissipationless spin currents are possible. Also, the addition of a magnetic field or a spin filter to the setup would be an interesting road to follow. In that way the nontrivial spin dependence highlighted by the presence of a spin-projected charge conductance could manifest in quantities that are easier to measure, such as the density of states or charge conductance.

[1] P. G. de Gennes, Boundary effects in superconductors, Rev. Mod. Phys. **36**, 225 (1964).

[2] F. Steglich, J. Aarts, C. D. Bredl, W. Lieke, D. Meschede, W. Franz, and H. Schäfer, Superconductivity in the Presence of Strong Pauli Paramagnetism: CeCu₂Si₂, Phys. Rev. Lett. **43**, 1892 (1979).

[3] L. J. Buchholtz and G. Zwicknagl, Identification of *p*-wave superconductors, Phys. Rev. B **23**, 5788 (1981).

[4] J. G. Bednorz and K. A. Müller, Possible high T_c superconductivity in the Ba–La–Cu–O system, Z. Phys. B: Condens. Matter **64**, 189 (1986).

[5] L. Fu and C. L. Kane, Superconducting Proximity Effect and Majorana Fermions at the Surface of a Topological Insulator, Phys. Rev. Lett. **100**, 096407 (2008).

[6] M. Sigrist and K. Ueda, Phenomenological theory of unconventional superconductivity, Rev. Mod. Phys. **63**, 239 (1991).

[7] Y. Maeno, S. Kittaka, T. Nomura, S. Yonezawa, and K. Ishida, Evaluation of spin-triplet superconductivity in Sr₂RuO₄, J. Phys. Soc. Jpn. **81**, 011009 (2012).

[8] M. Sigrist, Review on the chiral *p*-wave phase of Sr₂RuO₄, Prog. Theor. Phys. Suppl. **160**, 1 (2005).

[9] A. P. Schnyder, S. Ryu, A. Furusaki, and A. W. W. Ludwig, Classification of topological insulators and superconductors in three spatial dimensions, Phys. Rev. B **78**, 195125 (2008).

[10] C. Kallin and A. Berlinsky, Is Sr₂RuO₄ a chiral p-wave superconductor? J. Phys.: Condens. Matter **21**, 164210 (2009).

[11] M. Eschrig, Spin-polarized supercurrents for spintronics: A review of current progress, Rep. Prog. Phys. **78**, 104501 (2015).

[12] J. Linder and J. W. Robinson, Superconducting spintronics, Nat. Phys. **11**, 307 (2015).

[13] H. G. Suh, H. Menke, P. M. R. Brydon, C. Timm, A. Ramires, and D. F. Agterberg, Stabilizing even-parity chiral superconductivity in Sr₂RuO₄, Phys. Rev. Res. **2**, 032023(R) (2020).

[14] F. S. Bergeret, A. F. Volkov, and K. B. Efetov, Odd triplet superconductivity and related phenomena in superconductor-ferromagnet structures, Rev. Mod. Phys. **77**, 1321 (2005).

[15] Y. Tanaka, M. Sato, and N. Nagaosa, Symmetry and topology in superconductors–odd-frequency pairing and edge states–, J. Phys. Soc. Jpn. **81**, 011013 (2012).

[16] J. Linder and A. V. Balatsky, Odd-frequency superconductivity, Rev. Mod. Phys. **91**, 045005 (2019).

[17] J. Cayao, C. Triola, and A. M. Black-Schaffer, Odd-frequency superconducting pairing in one-dimensional systems, Eur. Phys. J.: Spec. Top. **229**, 545 (2020).

[18] *Non-centrosymmetric Superconductors: Introduction and Overview*, edited by E. Bauer and M. Sigrist, Lecture Notes in Physics Vol. 847 (Springer, Berlin, 2012).

[19] E. Bauer, G. Hilscher, H. Michor, C. Paul, E.-W. Scheidt, A. Gribanov, Y. Seropegin, H. Noël, M. Sigrist, and P. Rogl, Heavy Fermion Superconductivity and Magnetic Order in Noncentrosymmetric CePt₃Si, Phys. Rev. Lett. **92**, 027003 (2004).

[20] G. Amano, S. Akutagawa, T. Muranaka, Y. Zenitani, and J. Akimitsu, Superconductivity at 18 K in yttrium sesquicarbide system, Y₂C₃, J. Phys. Soc. Jpn. **73**, 530 (2004).

[21] T. Akazawa, H. Hidaka, H. Kotegawa, T. C. Kobayashi, T. Fujiwara, E. Yamamoto, Y. Haga, R. Settai, and Y. Ōnuki, Pressure-induced superconductivity in UIr, J. Phys. Soc. Jpn. **73**, 3129 (2004).

[22] K. Togano, P. Badica, Y. Nakamori, S. Orimo, H. Takeya, and K. Hirata, Superconductivity in the Metal Rich Li-Pd-B Ternary Boride, Phys. Rev. Lett. **93**, 247004 (2004).

[23] N. Tateiwa, Y. Haga, T. D. Matsuda, S. Ikeda, T. Yasuda, T. Takeuchi, R. Settai, and Y. Ōnuki, Novel pressure phase diagram of heavy fermion superconductor CePt₃Si investigated by ac calorimetry, J. Phys. Soc. Jpn. **74**, 1903 (2005).

[24] N. Kimura, K. Ito, K. Saitoh, Y. Umeda, H. Aoki, and T. Terashima, Pressure-Induced Superconductivity in Noncentrosymmetric Heavy-Fermion CeRhSi₃, Phys. Rev. Lett. **95**, 247004 (2005).

[25] I. Sugitani, Y. Okuda, H. Shishido, T. Yamada, A. Thamizhavel, E. Yamamoto, T. D. Matsuda, Y. Haga, T. Takeuchi, R. Settai, and Y. Ōnuki, Pressure-induced heavy-fermion superconductivity in antiferromagnet CeIrSi₃ without inversion symmetry, J. Phys. Soc. Jpn. **75**, 043703 (2006).

[26] F. Honda, I. Bonalde, K. Shimizu, S. Yoshiuchi, Y. Hirose, T. Nakamura, R. Settai, and Y. Ōnuki, Pressure-induced superconductivity and large upper critical field in the noncentrosymmetric antiferromagnet CeIrGe₃, Phys. Rev. B **81**, 140507 (2010).

[27] R. Settai, I. Sugitani, Y. Okuda, A. Thamizhavel, M. Nakashima, Y. Ōnuki, and H. Harima, Pressure-induced superconductivity in CeCoGe₃ without inversion symmetry, J. Magn. Magn. Mater. **310**, 844 (2007).

[28] E. Bauer, G. Rogl, X.-Q. Chen, R. T. Khan, H. Michor, G. Hilscher, E. Royanian, K. Kumagai, D. Z. Li, Y. Y. Li, R. Podloucky, and P. Rogl, Unconventional superconducting phase in the weakly correlated noncentrosymmetric Mo₃Al₂C compound, Phys. Rev. B **82**, 064511 (2010).

[29] W. Xie, P. Zhang, B. Shen, W. Jiang, G. Pang, T. Shang, C. Cao, M. Smidman, and H. Yuan, CaPtAs: A new noncentrosymmetric superconductor, Sci. China Phys. Mech. Astron. **63**, 237412 (2020).

[30] G. Annunziata, D. Manske, and J. Linder, Proximity effect with noncentrosymmetric superconductors, Phys. Rev. B **86**, 174514 (2012).

[31] Y. Tanaka, T. Kokkeler, and A. Golubov, Theory of proximity effect in $s + p$-wave superconductor junctions, Phys. Rev. B **105**, 214512 (2022).

[32] W. Belzig, F. K. Wilhelm, C. Bruder, G. Schön, and A. Zaikin, Quasiclassical Green's function approach to mesoscopic superconductivity, Superlattices Microstruct. **25**, 1251 (1999).

[33] V. Chandrasekhar, An introduction to the quasiclassical theory of superconductivity for diffusive proximity-coupled systems, in *The Physics of Superconductors*, edited by K.-H. Bennemann and J. Ketterson (Springer, Berlin, 2004), pp. 55–110.

[34] G. Eilenberger, Transformation of Gorkov's equation for type II superconductors into transport-like equations, Z. Phys. A **214**, 195 (1968).

[35] A. Larkin and Y. Ovchinnikov, Quasiclassical method in the theory of superconductivity, Zh. Eksp. Teor. Fiz. **55**, 2262 (1968) [Sov. Phys. JETP **28**, 1200 (1969)].

[36] K. D. Usadel, Generalized Diffusion Equation for Superconducting Alloys, Phys. Rev. Lett. **25**, 507 (1970).

[37] B. Josephson, Possible new effects in superconductive tunnelling, Phys. Lett. **1**, 251 (1962).

[38] B. Josephson, Coupled superconductors, Rev. Mod. Phys. **36**, 216 (1964).

[39] B. Josephson, Supercurrents through barriers, Adv. Phys. **14**, 419 (1965).

[40] A. I. Larkin and Y. U. N. Ovchinnikov, Nonlinear effects during the motion of vortices in superconductors, Zh. Eksp. Teor. Fiz. **73**, 7 (1977) [Sov. Phys. JETP **46**, 155 (1978)].

[41] A. Kastalsky, A. W. Kleinsasser, L. H. Greene, R. Bhat, F. P. Milliken, and J. P. Harbison, Observation of Pair Currents in Superconductor-Semiconductor Contacts, Phys. Rev. Lett. **67**, 3026 (1991).

[42] A. Volkov, A. Zaitsev, and T. Klapwijk, Proximity effect under nonequilibrium conditions in double-barrier superconducting junctions, Phys. C (Amsterdam) **210**, 21 (1993).

[43] A. Volkov, The proximity effect and subgap conductivity in superconductor-barrier-normal metal contacts, Phys. B (Amsterdam) **203**, 267 (1994).

[44] B. J. van Wees, P. de Vries, P. Magnée, and T. M. Klapwijk, Excess Conductance of Superconductor-Semiconductor Interfaces Due to Phase Conjugation Between Electrons and Holes, Phys. Rev. Lett. **69**, 510 (1992).

[45] Y. V. Nazarov, Circuit Theory of Andreev Conductance, Phys. Rev. Lett. **73**, 1420 (1994).

[46] S. Yip, Conductance anomalies for normal-metal–insulator–superconductor contacts, Phys. Rev. B **52**, 15504 (1995).

[47] V. Schmidt, *The Physics of Superconductors* (Springer, Berlin, 1997).

[48] Y. Tanaka and S. Kashiwaya, Anomalous charge transport in triplet superconductor junctions, Phys. Rev. B **70**, 012507 (2004).

[49] M. Eschrig, C. Iniotakis, and Y. Tanaka, Properties of interfaces and surfaces in non-centrosymmetric superconductors, in *Noncentrosymmetric Superconductors*, edited by E. Bauer and M. Sigrist, Lecture Notes in Physics Vol. 847 (Springer, Berlin, 2012), pp. 313–357.

[50] P. Gentile, C. Noce, A. Romano, G. Annunziata, J. Linder, and M. Cuoco, Odd-frequency triplet pairing in mixed-parity superconductors, arXiv:1109.4885.

[51] Y. Rahnavard, D. Manske, and G. Annunziata, Magnetic Josephson junctions with noncentrosymmetric superconductors, Phys. Rev. B **89**, 214501 (2014).

[52] V. Mishra, Y. Li, F.-C. Zhang, and S. Kirchner, Effects of spin-orbit coupling in superconducting proximity devices: Application to $CoSi_2/TiSi_2$ heterostructures, Phys. Rev. B **103**, 184505 (2021).

[53] Y. Tanaka, Y. V. Nazarov, and S. Kashiwaya, Circuit Theory of Unconventional Superconductor Junctions, Phys. Rev. Lett. **90**, 167003 (2003).

[54] Y. V. Nazarov, Novel circuit theory of Andreev reflection, Superlattices Microstruct. **25**, 1221 (1999).

[55] Y. Tanaka and A. A. Golubov, Theory of the Proximity Effect in Junctions with Unconventional Superconductors, Phys. Rev. Lett. **98**, 037003 (2007).

[56] Y. Tanaka, Y. V. Nazarov, A. A. Golubov, and S. Kashiwaya, Theory of charge transport in diffusive normal metal/unconventional singlet superconductor contacts, Phys. Rev. B **69**, 144519 (2004).

[57] Y. Tanaka, S. Kashiwaya, and T. Yokoyama, Theory of enhanced proximity effect by midgap Andreev resonant state

in diffusive normal-metal/triplet superconductor junctions, Phys. Rev. B **71**, 094513 (2005).

[58] Y. Asano, Y. Tanaka, A. A. Golubov, and S. Kashiwaya, Conductance Spectroscopy of Spin-Triplet Superconductors, Phys. Rev. Lett. **99**, 067005 (2007).

[59] T. Yokoyama, Y. Tanaka, and A. A. Golubov, Resonant proximity effect in normal metal/diffusive ferromagnet/superconductor junctions, Phys. Rev. B **73**, 094501 (2006).

[60] Y. Sawa, T. Yokoyama, Y. Tanaka, and A. A. Golubov, Quasiclassical Green's function theory of the Josephson effect in chiral *p*-wave superconductor/diffusive normal metal/chiral *p*-wave superconductor junctions, Phys. Rev. B **75**, 134508 (2007).

[61] S.-I. Suzuki, A. A. Golubov, Y. Asano, and Y. Tanaka, Effects of phase coherence on local density of states in superconducting proximity structures, Phys. Rev. B **100**, 024511 (2019).

[62] S.-I. Suzuki, A. A. Golubov, Y. Asano, and Y. Tanaka, Quasiparticle spectrum in mesoscopic superconducting junctions with weak magnetization, in *Proceedings of the International Conference on Strongly Correlated Electron Systems (SCES2019)*, JPS Conference Proceedings Vol. 30 (Physical Society of Japan, Tokyo, 2020), p. 011045.

[63] T. Kokkeler, Usadel equation for a four terminal junction, Master's thesis, University of Twente, 2021.

[64] G. E. Volovik, *The Universe in a Helium Droplet*, International Series of Monographs on Physics Vol. 117 (Oxford University Press, Oxford, 2003).

[65] C. Iniotakis, N. Hayashi, Y. Sawa, T. Yokoyama, U. May, Y. Tanaka, and M. Sigrist, Andreev bound states and tunneling characteristics of a noncentrosymmetric superconductor, Phys. Rev. B **76**, 012501 (2007).

[66] X.-L. Qi, T. L. Hughes, S. Raghu, and S.-C. Zhang, Time-Reversal-Invariant Topological Superconductors and Superfluids in Two and Three Dimensions, Phys. Rev. Lett. **102**, 187001 (2009).

[67] Y. Tanaka, T. Yokoyama, A. V. Balatsky, and N. Nagaosa, Theory of topological spin current in noncentrosymmetric superconductors, Phys. Rev. B **79**, 060505 (2009).

[68] M. Matsumoto and M. Sigrist, Quasiparticle states near the surface and the domain wall in a $p_x \pm ip_y$-wave superconductor, J. Phys. Soc. Jpn. **68**, 994 (1999).

[69] N. Read and D. Green, Paired states of fermions in two dimensions with breaking of parity and time-reversal symmetries and the fractional quantum Hall effect, Phys. Rev. B **61**, 10267 (2000).

[70] A. Furusaki, M. Matsumoto, and M. Sigrist, Spontaneous Hall effect in a chiral *p*-wave superconductor, Phys. Rev. B **64**, 054514 (2001).

[71] See Supplemental Material at http://link.aps.org/supplemental/10.1103/PhysRevResearch.5.L012022 for an explicit calculation.

[72] P. Burset, F. Keidel, Y. Tanaka, N. Nagaosa, and B. Trauzettel, Transport signatures of superconducting hybrids with mixed singlet and chiral triplet states, Phys. Rev. B **90**, 085438 (2014).

[73] S.-P. Chiu, C. Tsuei, S.-S. Yeh, F.-C. Zhang, S. Kirchner, and J.-J. Lin, Observation of triplet superconductivity in $CoSi_2/TiSi_2$ heterostructures, Sci. Adv. **7**, eabg6569 (2021).